Kinetics of the Reactions of CH_2Cl, CH_3CHCl, and CH_3CCl_2 Radicals with Cl_2 in the Temperature Range 191−363 K†

Matti P. Rissanen, Arkke J. Eskola,‡ and Raimo S. Timonen*

Laboratory of Physical Chemistry, University of Helsinki, P.O. Box 55 (A.I. Virtasen aukio 1), Helsinki FIN-00014, Finland

Received: September 30, 2009; Revised Manuscript Received: December 22, 2009

The kinetics of three chlorinated free radical reactions with Cl_2 have been studied in direct time-resolved measurements. Radicals were produced in low initial concentrations by pulsed laser photolysis at 193 nm, and the subsequent decays of the radical concentrations were measured under pseudo-first-order conditions using photoionization mass spectrometer (PIMS). The bimolecular rate coefficients of the $CH_3CHCl + Cl_2$ reaction obtained from the current measurements exhibit negative temperature dependence and can be expressed by the equation $k(CH_3CHCl + Cl_2) = ((3.02 \pm 0.14) \times 10^{-12})(T/300\ K)^{-1.89\pm0.19}$ cm^3 molecule^{-1} s^{-1} (1.7−5.4 Torr, 191−363 K). For the $CH_3CCl_2 + Cl_2$ reaction the current results could be fitted with the equation $k(CH_3CCl_2 + Cl_2) = ((1.23 \pm 0.02) \times 10^{-13})(T/300\ K)^{-0.26\pm0.10}$ cm^3 molecule^{-1} s^{-1} (3.9−5.1 Torr, 240−363 K). The measured rate coefficients for the $CH_2Cl + Cl_2$ reaction plotted as a function of temperature show a minimum at about $T = 240$ K: first decreasing with increasing temperature and then, above the limit, increasing with temperature. The determined reaction rate coefficients can be expressed as $k(CH_2Cl + Cl_2) = ((2.11 \pm 1.29) \times 10^{-14}) \exp(773 \pm 183\ K/T)(T/300\ K)^{3.26\pm0.67}$ cm^3 molecule^{-1} s^{-1} (4.0−5.6 Torr, 201−363 K). The rate coefficients for the $CH_3CCl_2 + Cl_2$ and $CH_2Cl + Cl_2$ reactions can be combined with previous results to obtain: $k_{combined}(CH_3CCl_2 + Cl_2) = ((4.72 \pm 1.66) \times 10^{-15}) \exp(971 \pm 106\ K/T)(T/300\ K)^{3.07\pm0.23}$ cm^3 molecule^{-1} s^{-1} (3.1−7.4 Torr, 240−873 K) and $k_{combined}(CH_2Cl + Cl_2) = ((5.18 \pm 1.06) \times 10^{-14}) \exp(525 \pm 63\ K/T)(T/300\ K)^{2.52\pm0.13}$ cm^3 molecule^{-1} s^{-1} (1.8−5.6 Torr, 201−873 K). All the uncertainties given refer only to the 1σ statistical uncertainties obtained from the fitting, and the estimated overall uncertainty in the determined bimolecular rate coefficients is about ±15%.

Introduction

Chlorinated alkyl free radicals are common intermediates in combustion and atmospheric chemistry.[1,2] They are frequently involved through the use of chlorinated solvents and reagents in industrial synthesis and also in smaller scale processes.[3−6] They are important intermediates in the incineration of hazardous wastes,[1,7] can enhance soot formation in fuel-rich oxidation,[8] and play a role in stratospheric ozone depletion.[9]

Chlorine (Cl_2) is one of the most produced materials in the world, and its common uses in industry are numerous. It is used, for example, in bleaching paper and cloths, cleaning waters, manufacturing pesticides, drugs, rubber and plastics, and so on.[10,11] The high reactivity of Cl_2 prevents its occurrence as a free molecule in the universe, and in our environment it readily forms chlorinated radicals through sunlight photolysis.[12] Because chlorinated radicals and chlorine molecules are present together in many different environments, the rates and the mechanisms of their mutual reactions are of industrial as well as of scientific interest. Here we present the results of direct kinetic measurements of the rate coefficients of three free radical reactions with molecular chlorine

$$CH_2Cl + Cl_2 \rightarrow \text{products} \quad (1)$$

$$CH_3CHCl + Cl_2 \rightarrow \text{products} \quad (2)$$

$$CH_3CCl_2 + Cl_2 \rightarrow \text{products} \quad (3)$$

These reactions have all been studied previously, but the temperature range ($T = 191$−295 K) measured in this work has not been an object of previous kinetic studies for the title reactions.

Johnston et al.[13] and Bell et al.[14] have studied the $CH_2Cl + Cl_2$ reaction by means of transition state theory (TST) and BEBO theory, respectively. Seetula et al. measured the $CH_2Cl + Cl_2$ ($T = 295$−873 K, $p = 1.8$−5.3 Torr)[15,16] and $CH_3CCl_2 + Cl_2$ ($T = 414$−873 K, $p = 3.1$−7.4 Torr)[15] reaction rate coefficients, using similar LP-PIMS setup with a different temperature controlling system than is used in the present work, and also studied the reaction transition states with ab initio methods.[15] This work was performed to extend the temperature ranges in which $CH_2Cl + Cl_2$ and $CH_3CCl_2 + Cl_2$ reactions have been measured to lower temperatures, which have not been previously attained.

Kinetics of the $CH_3CHCl + Cl_2$ reaction at 298 K has been measured directly by Knyazev et al.[17] using LP-PIMS at low pressures (2−11 Torr). Kaiser et al.[18,19] have studied the $CH_3CHCl + Cl_2$ reaction with respect to the $CH_3CHCl + O_2$ reaction using relative rate method and initiating the reactions using 351 nm photolysis of Cl_2 in a reaction cell ($T = 298$ K, 700 Torr of N_2) and employing absorption spectroscopy for product analysis. Dobis and Benson[20] measured the kinetics of

† Part of the special section "30th Free Radical Symposium".

* Corresponding author, raimo.timonen@helsinki.fi.

‡ Current address: School of Chemistry, University of Leeds, Leeds LS2 9JT, U.K.

10.1021/jp909419v
Published on Web 02/05/2010

$CH_3CHCl + Cl_2$ reaction under very low pressure conditions (VLPR-method) at room temperature.

Experimental Section

Details of the experimental apparatus and the procedures used to measure the bimolecular reaction rate coefficients of the studied radical−molecule reactions have been described previously,[21] and only an overview is given here. The reactions were studied in a temperature-controlled stainless steel flow tube reactor (8 mm i.d., coated with Halocarbon Wax, Supelco) coupled to a photoionization mass spectrometer. Reactions were initiated by producing the radicals homogeneously along the reactor with unfocused exciplex laser (ASX-750) photolysis of suitable precursors at 193 nm. The gas flow velocity inside the reactor was about 5 ms^{-1} which ensured that the repetitive photolysis at 5 Hz always photolyzed a fresh gas mixture. In every measurement the molecular reactant was in large excess over initial radical concentration ($[Cl_2] \gg [R]_0$) resulting in pseudo-first-order decay kinetics with respect to radical concentration.

The change in the radical concentration as a function of time was continuously measured by taking a portion of the gas mixture through a small hole in the wall of the reactor. The sampled gas was formed into a beam by a conical skimmer and ionized with a radiation from a resonance gas lamp (Cl_2 with CaF_2 windows, 8.9−9.1 eV). The ion of the radical was mass selected in a quadropole mass filter (Extrel, C-50/150-QC/19 mm rods) and detected with an electron multiplier. The resulting single ion counts were recorded with a multichannel scaler (EG&G Ortec MCS plus). Typically 1500−20000 laser pulses were needed for averaging before an exponential function $\{[R]_t = [R]_0 \exp(-k't)\}$ was fit to the measured radical signal to obtain the pseudo-first-order decay rate coefficient (k') as the initial radical concentration ($[R]_0$) decreases to concentration $[R]_t$ at time t.

Exciplex laser photolysis at 193 nm was used to produce the radicals for the kinetic measurements. The chloromethyl radicals were produced in the photolysis of CH_2ClBr

$$CH_2ClBr + h\nu(193\ nm) \rightarrow CH_2Cl + Br \quad (4)$$
$$\rightarrow \text{other products}$$

The 1-chloroethyl radicals were generated in the photolysis of 1,1-dichloroethane. The primary dissociation channel is the C−Cl bond fission

$$CH_3CHCl_2 + h\nu(193\ nm) \rightarrow CH_3CHCl + Cl \quad (5)$$
$$\rightarrow \text{other products}$$

The dichloroethyl radicals were produced from methyl chloroform

$$CH_3CCl_3 + h\nu(193\ nm) \rightarrow CH_3CCl_2 + Cl \quad (6)$$
$$\rightarrow \text{other products}$$

Initial radical concentrations in the measurements were calculated with the known absorption cross section (CH_2ClBr and CH_3CCl_3),[2] laser fluence, and the concentration of the precursor, or it was estimated[21] from the precursor decomposition signal (CH_3CHCl_2). Calculated initial radical concentrations were between 0.5 and 6 × 10^{11} molecules cm^{-3} in all measurements. Mostly it was close to 1 × 10^{11} molecules cm^{-3} to avoid interference from second-order radical reactions. No dependences of the rate coefficients on initial radical concentrations were observed in these experiments.

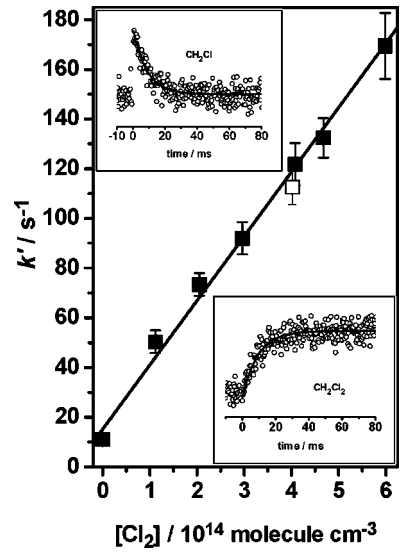

Figure 1. A plot of the measured pseudo-first-order rate coefficients as a function of reactant concentration used to obtain the bimolecular reaction rate coefficient of the $CH_2Cl + Cl_2$ reaction under the experimental conditions: $T = 267$ K, $[He] = 1.28 \times 10^{17}$ molecules cm^{-3}, 8 mm reactor with HW coating, laser fluence ≈ 30 mJ cm^{-2}. Also included in insets are the CH_2Cl radical decay and the corresponding CH_2Cl_2 ($m/z = 88$) product formation signals, respectively. They were measured under the conditions of the hollow square in the plot: $[Cl_2] = 4.02 \times 10^{14}$ molecules cm^{-3}. The fitted first-order exponential lines in the radical and product signals give the pseudo-first-order rate coefficients under these experimental conditions: $k_d'(CH_2Cl) = 113 \pm 7\ s^{-1}$ and $k_f'(CH_2Cl_2) = 107 \pm 6\ s^{-1}$.

At the beginning (and in the end) of measurements the decay rate of the produced radical concentration was measured without added reactant. The radical loss rate obtained this way corresponds to all the other losses of the radical in the system, except for the loss in the reaction under study, and was termed as the wall rate coefficient (k_w'). After this the reactant gas (Cl_2) was introduced to the carrier gas flow in different concentrations, which were determined by measuring the pressure change in a known volume, and the respective pseudo-first-order rate coefficients of the radical loss were measured. When the measured first-order radical decay rate coefficients (k') were plotted as a function of used reactant concentration $[Cl_2]$, the bimolecular reaction rate coefficient $k(R + Cl_2)$ could be obtained from the slope of the plot according to the $k' = k_{wall} + k(R + Cl_2)[Cl_2]$ equation. An example of this procedure is shown in Figure 1 for the $CH_2Cl + Cl_2$ reaction with the measured radical decay and product formation signals in the insets.

Products of the studied reactions were sought by applying different ionization energies by changing the light-emitting gas and the window material of the resonance gas lamp. Lamps and windows employed to ionize and detect radicals and products were: a Cl lamp with CaF_2 windows (8.9−9.1 eV) for CH_2Cl, CH_3CHCl, and CH_3CCl_2; a H lamp with MgF_2 windows (10.2 eV) for CHCl, CH_2Cl, $CHCl_2$, CCl_2, CH_2Cl_2, CH_2CCl, CH_3CHCl, CH_3CHCl_2, CH_3CCl_2; and a Ne lamp with a CHS (collimated hole structure) plate (16.7 and 16.9 eV) for Cl, HCl, Cl_2, CCl_2, CH_2Cl_2, CH_2CHCl, CH_2CCl_2, CH_2CCl_3, and CH_3CCl_3. All the experiments to study the kinetics of the reactions were performed using a chlorine lamp for ionization. However, some radical signals were measured with a hydrogen

TABLE 1: Results and Conditions of the Experiments Used to Measure Reactions R + Cl_2 → Products (R = CH_2Cl, CH_3CHCl, and CH_3CCl_2)[a]

T/K	[He]/10^{17} molecules cm^{-3}	[Cl_2]/10^{13} molecules cm^{-3}	k [b]/10^{-13} cm^3 molecule^{-1} s^{-1}	k'/s^{-1}	k_{wall}/s^{-1}
R = CH_2Cl, ($CH_2Cl + Cl_2$ → products)					
Current data:					
$k = ((2.11 \pm 1.29) \times 10^{-14}) \exp((773 \pm 183)\ \mathrm{K}/T)(T/300\ \mathrm{K})^{3.26\pm0.67}$ cm^3 molecule^{-1} s^{-1}					
Current and previously measured[15] data combined:					
$k = ((5.18 \pm 1.06) \times 10^{-14}) \exp((525 \pm 63)\ \mathrm{K}/T)(T/300\ \mathrm{K})^{2.52\pm0.13}$ cm^3 molecule^{-1} s^{-1}					
201	1.36	10.9−60.6	2.67 ± 0.12	57.6−175.9	12
221	1.30	10.2−61.1	2.62 ± 0.16	51.1−165.8	9
241	1.27	9.55−56.5	2.48 ± 0.14	58.0−163.4	14
254	1.30	9.69−51.1	2.69 ± 0.05	38.9−153.6	14
267	1.28	11.2−59.8	2.59 ± 0.08	50.4−169.4	11
298	1.29	10.2−42.8	2.66 ± 0.14	42.3−121.2	9
298	1.80	12.4−58.2	2.87 ± 0.09	60.2−186.7	20
336	1.29	21.1−58.9	2.99 ± 0.15	83.9−190.9	19
363	1.28	8.72−57.7	3.35 ± 0.11	57.3−206.0	15
R = CH_3CHCl, ($CH_3CHCl + Cl_2$ → products)					
$k(CH_3CHCl + Cl_2) = ((3.02 \pm 0.14) \times 10^{-12})(T/300\ \mathrm{K})^{-1.89\pm0.19}$ cm^3 molecule^{-1} s^{-1}					
191	1.38	0.45−1.61	81.8 ± 2.15	76.7−176.2	46
201	1.41	0.62−4.12	61.0 ± 3.45	77.1−283.8	29
221	1.43	0.57−3.12	59.9 ± 4.24	75.3−222.9	35
241	1.39	1.10−5.29	40.1 ± 3.06	80.2−226.4	22
267	1.39	0.99−8.20	32.4 ± 2.09	82.5−294.9	21
298	0.54	1.05−4.81	31.4 ± 2.23	48.9−172.6	14
298	1.74	1.12−5.30	26.3 ± 2.35	59.6−149.1	11
298	1.66	1.14−4.39	29.3 ± 3.33	68.6−179.1	28
336	1.28	0.95−5.76	25.7 ± 2.90	39.4−171.6	26
363	1.27	1.64−8.08	24.0 ± 2.19	48.2−210.3	11
R = CH_3CCl_2, ($CH_3CCl_2 + Cl_2$ → products)					
Current data:					
$k = ((1.23 \pm 0.02) \times 10^{-13})(T/300\ \mathrm{K})^{-0.26\pm0.10}$ cm^3 molecule^{-1} s^{-1}					
Current and previously measured[15] data combined:					
$k = ((4.72 \pm 1.66) \times 10^{-15}) \exp((971 \pm 106)\ \mathrm{K}/T)(T/300\ \mathrm{K})^{3.07\pm0.23}$ cm^3 molecule^{-1} s^{-1}					
240	1.67	19.1−89.0	1.29 ± 0.05	47.5−136.4	22
243	1.66	17.2−65.9	1.38 ± 0.06	40.7−109.5	18
266	1.68	22.1−75.0	1.20 ± 0.07	50.8−102.7	17
298	1.27	21.2−65.8	1.24 ± 0.09	43.9−96.9	18
298	1.65	19.0−106	1.18 ± 0.05	37.1−140.8	18
336	1.28	20.3−75.4	1.21 ± 0.14	38.7−99.8	14
336	1.26	19.5−58.6	1.17 ± 0.06	37.3−75.6	7
363	1.26	21.5−111	1.21 ± 0.12	30.1−129.0	5

[a] Range of precursor concentrations used: (0.77−3.0) × 10^{13} molecules cm^{-3} for CH_2ClBr, (1.87−6.95) × 10^{12} molecules cm^{-3} for CH_3CHCl_2 and (0.07−1.42) × 10^{13} molecules cm^{-3} for CH_3CCl_3. [b] Statistical uncertainties shown are 1σ. Estimated overall uncertainty in the measured bimolecular rate coefficients is about ±15%.

lamp for ionization for comparison. No differences in the measured pseudo-first-order kinetics were observed.

Precursors bromochloromethane (CH_2ClBr, Fluka, 98%), 1,1-dichloroethane (CH_3CHCl_2, Aldrich, 97%), 1,1,1-trichloroethane (CH_3CCl_3, Aldrich, 99%), and reagent chlorine gas (Cl_2, Messer-Griesheim, 99.8%) were degassed prior to use by several freeze−pump−thaw cycles. The carrier gas (He, Messer-Griesheim, 99.9996%) was used as supplied.

Results and Discussion

The results of the performed measurements and the corresponding experimental conditions are presented in Table 1. The determined bimolecular R + Cl_2 reaction rate coefficients together with the results from previous studies are shown as a function of temperature on a double-logarithmic plot in Figure 2. For the current results of the $CH_3CHCl + Cl_2$ and $CH_3CCl_2 + Cl_2$ reactions, the rate coefficients' dependence on temperature can be expressed by the equation: $k = k_{300K}(T/300\ \mathrm{K})^n$, where T is temperature in K, k_{300K} is the room temperature (T = 300 K) rate coefficient, and n is the coefficient describing temperature dependence. The rate coefficients measured for the $CH_2Cl + Cl_2$ reaction and for the CH_3CCl_2 reaction with Cl_2 combined with previous data,[15,16] show a discernible curvature in their double-logarithmic plots and a temperature-dependent pre-exponential factor had to be used for a better fit. Three parameter fits of the modified Arrhenius equation $k = \hat{A} \exp(B/T)(T/300\ \mathrm{K})^m$, where T is temperature in K, and $\hat{A}$, B, and m are fitting parameters, are given separately for the current data and also for the whole data including previously measured values by Seetula et al.[15,16] These obtained expressions for the rate coefficients can be found in Table 1. The preferred fits, i.e., the fits with widest experimental range, have been included in Figure 2.

The only product observed for the reactions studied was CH_2Cl_2 (m/z = 88) in $CH_2Cl + Cl_2$ reaction in agreement with the previous work by Seetula et al.[15,16] The measured signal is shown in the inset of Figure 1 together with the corresponding CH_2Cl radical decay profile. The exponential fits to the signals

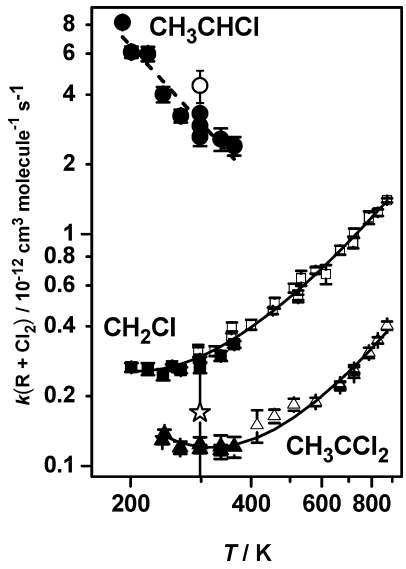

Figure 2. Double-logarithmic plot of the determined R + Cl_2 bimolecular reaction rate coefficients shown as a function of temperature. Included are the previously measured values for the CH_2Cl (hollow squares) and CH_3CCl_2 (hollow triangles) radical reactions with Cl_2 measured by Seetula et al.[15,16] and the measurements of Knyazev et al.[17] (hollow circle) and Benson and Dobis[20] (hollow star) on $CH_3CHCl + Cl_2$ reaction. Current results are indicated with solid symbols. The temperature dependences of the $CH_2Cl + Cl_2$ and $CH_3CCl_2 + Cl_2$ reactions are fitted according to expression $k = \hat{A}\exp(B/T)(T/300\text{ K})^n$. For the $CH_3CHCl + Cl_2$ reaction rate coefficients the temperature dependence is fitted by equation $k = k_{300K}(T/300\text{ K})^n$.

correspond to the pseudo-first-order decay ($k_d'(CH_2Cl) = 113 \pm 7\ s^{-1}$) and formation ($k_f'(CH_2Cl_2) = 107 \pm 6\ s^{-1}$) rate coefficients and their similar values within the statistical uncertainties of the fits are taken as an indication that the signals are formed in the same reaction.

The $CH_2Cl + Cl_2$ reaction has been studied before by Johnston et al.[13] using transition state theory and Bell et al.[14] using the BEBO method. These early theoretical studies give rate coefficients that differ orders of magnitude from the current results ($k_{300K} = 3.5 \times 10^{-15}$ cm^3 molecule^{-1} s^{-1} with TST[13] and $k_{300K} = 5.9 \times 10^{-17}$ cm^3 molecule^{-1} s^{-1} with BEBO,[14] respectively) and will not be considered here afterward. Direct, more recent studies have been performed by Seetula et al.[15,16] ($T = 295-873$ K, $p = 1.8-5.3$ Torr) with essentially similar LP-PIMS setup as was used in the present study. The agreement between these values and the bimolecular rate coefficients obtained in this work is excellent as can be seen in Figure 2. The rate coefficients measured by Seetula et al.[15,16] are presented with hollow squares, and the results from the current work are indicated with filled squares. Considering only the current results, the rate coefficients of the $CH_2Cl + Cl_2$ reaction can be expressed as a function of temperature with equation $k(CH_2Cl + Cl_2) = ((2.11 \pm 1.29) \times 10^{-14})\exp(773 \pm 183\text{ K}/T)(T/300\text{ K})^{3.26\pm0.67}$ cm^3 molecule^{-1} s^{-1}. Taking the previous results into account, the expression becomes: $k_{combined}(CH_2Cl + Cl_2) = ((5.18 \pm 1.06) \times 10^{-14})\exp(525 \pm 63\text{ K}/T)(T/300\text{ K})^{2.52\pm0.13}$ cm^3 molecule^{-1} s^{-1}. Seetula et al.[15] also studied the reaction transition states by ab initio calculations and found that as the electron density of the radical center decreases the transition state of the R + Cl_2 reaction becomes tighter.

The room temperature rate coefficient of the $CH_3CHCl + Cl_2$ reaction has been measured by Knyazev et al.,[17] by Kaiser et al.[18,19] and by Dobis and Benson.[20] Knyazev et al.[17] measured it at low pressures (2−11 Torr) with a similar method as in the present work and obtained $k_{298K}(CH_3CHCl + Cl_2) = (4.37 \pm 0.70) \times 10^{-12}$ cm^3 molecule^{-1} s^{-1} in reasonably good agreement with the current value $k_{300K}(CH_3CHCl + Cl_2) = (3.02 \pm 0.45) \times 10^{-12}$ cm^3 molecule^{-1} s^{-1}. Kaiser et al.[18,19] measured reaction 2 indirectly in a relative rate determination using 351 nm light to photolyze Cl_2 in order to initiate the reactions in a reaction cell ($T = 298$ K and 700 Torr N_2), using absorption spectroscopy for analysis method and $CH_3CHCl + O_2$ as a reference reaction. They obtained 0.42 as a ratio of the $CH_3CHCl + Cl_2$ and $CH_3CHCl + O_2$ reaction rate coefficients. Dobis and Benson[20] studied the $CH_3CHCl + Cl_2$ reaction with a VLPR technique in the millitorr pressure range and obtained $k_{298K}(CH_3CHCl + Cl_2) = (1.7 \pm 1.0) \times 10^{-13}$ cm^3 molecule^{-1} s^{-1} in a gross disagreement with the current result.

The $CH_3CCl_2 + Cl_2$ reaction has been studied by Seetula et al.[15] both experimentally to measure the kinetics of the reaction and also using an ab initio calculation to locate the reaction transition states and energies. The rate coefficients measured by Seetula et al.[15] ($T = 414-873$ K, $p = 3.1-7.4$ Torr) are presented with hollow triangles in Figure 2, together with the current results (filled triangles). The agreement between the two set of results is good. The expression: $k(CH_3CCl_2 + Cl_2) = ((1.23 \pm 0.02) \times 10^{-13})(T/300\text{ K})^{-0.26\pm0.10}$ cm^3 molecule^{-1} s^{-1} fits well to the data measured in this work. When previous values[15] are taken into account, a two-parameter fit cannot give an adequate description of the temperature dependence and a three-parameter fit is used instead: $k_{combined}(CH_3CCl_2 + Cl_2) = ((4.72 \pm 1.66) \times 10^{-15})\exp(971 \pm 106\text{ K}/T)(T/300\text{ K})^{3.07\pm0.23}$ cm^3 molecule^{-1} s^{-1}.

The rate coefficients of the CH_3CHCl radical reaction with Cl_2 exhibit a negative temperature dependence, which is notably different from the other two title reactions. The CH_3CHCl radical is also significantly more reactive toward Cl_2 than the other radicals studied in this work; at room temperature, it is about 10 times more reactive than CH_2Cl and about 20 times more than CH_3CCl_2. It should, however, be pointed out that the rate coefficients of $CH_2Cl + Cl_2$ and $CH_3CCl_2 + Cl_2$ reactions also possess negative temperature dependences below a certain temperature. For the CH_3CCl_2 radical the changing temperature is about $T = 340$ K and for the CH_2Cl radical about $T = 240$ K as seen in Figure 2. An intriguing question is whether the higher reactivity of CH_3CHCl radicals, than the other radicals studied in this work, is connected to its strong negative temperature dependence. Interesting information would be the value of $k(CH_3CHCl + Cl_2)$ at temperatures 600−800 K. Unfortunately, we are not currently able to reach those temperatures.

The temperature dependence of the $CH_3CHCl + Cl_2$ reaction rate coefficients shows a slight deviation from linearity on a logarithmic scale. Nevertheless, the aforementioned equation ($k = k_{300K}(T/300\text{ K})^n$) can still be used to properly describe the temperature dependence.

It seems obvious that CH_3CCl_2 radical has lower reactivity toward Cl_2 than CH_3CHCl. The same can be expected for CH_2Cl, although the reasons for the behavior in reactivity can be different. In the CH_3CCl_2 case, the radical site is hardest to attack because of the sterical hindrance of the two relatively large Cl atoms and a methyl group attached to it; this could make the reactivity lower compared to CH_2Cl. Because of the electron-withdrawing inductive effect of the halogen atoms in the CH_3CCl_2 radical, the radical site is more electron deficient than in CH_2Cl and CH_3CHCl. This can cause the lower reactivity compared to CH_3CHCl and CH_2Cl radicals. In the CH_3CHCl

radical, the electron density of the radical site should be higher than that in the CH_2Cl radical due to the methyl group's ability to serve as an electron donor. Therefore the reactivity of CH_3CHCl should be even higher than the reactivity of CH_2Cl, and the 10-fold difference in the room temperature reaction rate coefficient is noteworthy to be pointed out.

The reactivity differences among radical−molecule reactions toward a common reactant have been related to readily obtainable radical properties by making correlations of the observed rate coefficients against a chosen molecular property, to gain understanding about the underlying reasons for different reactivity. Linear correlations have been sought by making free energy plots for the reactions under study.[22] The logarithm of the room temperature rate coefficient is usually taken as a measure of the free energy of activation in similar types of reactions and is plotted against different radical properties. One example of such a procedure is to plot the logarithm of the room temperature rate coefficient ($\log(k_{300K})$) of the radical−molecule reaction against the electron affinity of the molecular reagent (EA(reactant)) subtracted from the ionization potential of the radical (IP(R)); [$\log(k_{300K})$ vs (IP(R) − EA(reactant))]. Paltenghi et al.[23] observed that this expression provides a good simultaneous correlation for oxygen and ozone reactions with alkyl radicals, instead of just correlating the logarithm of reaction rate coefficients with the ionization potential of the alkyl radicals (IP(R)) in one set of reactions. Another such example is to plot the $\log(k_{300K})$ for the radical−molecule reaction against Δ*Electronegativity* of the reactive radical, which is given in an arbitrary scale based on the simple sum of Pauling electronegativities[24,25] of the substituent atoms/groups. Δ*Electronegativity* of the radical is used for estimating the electron-withdrawing inductive effects of the substituents in the radical center. This scale was first introduced by Thomas[26] and transported to gas kinetics by Gutman and co-workers[16,27] who found it to be useful in explaining the observed differences in the rate coefficients of the methyl and halogenated methyl radical reactions with HI. The similar linear relationship was observed to hold for larger alkyl radicals when a group electronegativity value of 1.82 was assigned to the methyl group as a substituent.[27] It was also shown to correlate linearly with the rate coefficients of the R + Cl_2[16] and R + Br_2[28] reactions.

Two of these linear correlations were observed to hold for the current and selected similar R + Cl_2 reactions and they are shown in parts a and b of Figure 3. The room temperature rate coefficients are plotted against radicals' Δ*Electronegativity*(R) (Figure 3a) and electron affinity EA(R) (Figure 3b) on semilogarithmic plots. A good linear correlation spanning almost 6 orders of magnitude can be recognized in the plots. In Figure 3a the Δ*Electronegativities*(R) of the fluorinated radicals have been calculated using an effective electronegativity value 2.8 for isolated fluorine atom (instead of Paulings' value 3.98) to have them fit into the same correlation as has been discussed previously.[16] For the methyl group, an electronegativity value 1.82 was used, as has been briefly discussed above.

As seen in Figure 3a, the rates of R + Cl_2 reactions are affected by the electron densities in the radical centers; the rate of the reaction decreases together with decreasing electron density. For example a Cl atom, or halogen atoms in general, when substituted in the radical center withdraw electrons from the center and decrease the electron density. Chlorine molecule has a large electron affinity ($EA(Cl_2) \approx 2.40$ eV[29]) and consequently when electron density is higher in the radical center, as it is for alkyl substituted radicals, the rates of R + Cl_2 reactions are enhanced (Figure 3a). This could also suggest that the more loosely the electron is bound to the radical (lower the ionization energy of the radical) the faster the reaction rate should be, i.e., rate coefficients of these reactions should correlate with IE(R). However, this correlation was not observed.

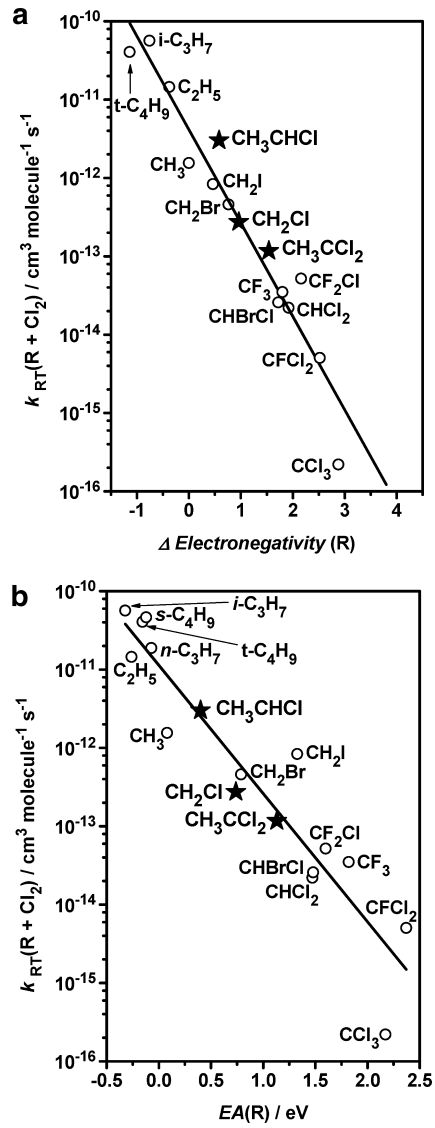

Figure 3. (a) Δ*Electronegativity* of the radical (R) plotted against the room temperature (RT = 298 ± 3 K) rate coefficient in current and selected R + Cl_2 reactions. Electronegativities were taken from Pauling,[24,25] and an electronegativity value of 1.82 was assigned to the methyl group in accordance with ref 27. Fluorinated radicals have been included to the correlation by assigning an effective electronegativity value of 2.8 to a fluorine atom as a substituent, as was briefly noted in the text and discussed in ref 16. The rate coefficients for the selected R + Cl_2 reactions were taken from CH_3,[30] CF_3,[31] CCl_3,[32] CHBrCl and $CHCl_2$,[15] CH_2Br and CH_2I,[16] CF_2Cl and $CFCl_2$,[33] C_2H_5, *n*-C_3H_7, and *n*-C_4H_9,[34] *s*-C_4H_9,[35,36] and *i*-C_3H_7 and *t*-C_4H_9.[37] The line in the picture is an unweighted, linear least-squares fit to the data. The current results are indicated by star symbols. (b) Electron affinity of the radical (R) plotted against the room temperature (RT = 298 ± 3 K) rate coefficient in current and selected R + Cl_2 reactions. Electron affinities were taken from ref 29 except for CH_2I[38] and for CHBrCl.[39] In the case of substituted ethyl radicals, the EA of the radical was unavailable and was estimated with the help of ref 40, e.g., for CH_3CCl_2: $EA(CH_3CCl_2) = EA(CH_3CH_2) + (EA(CHCl_2) - EA(CH_3))$. The rate coefficients for the selected R + Cl_2 reactions were taken from: CH_3,[30] CF_3,[31] CCl_3,[32] CHBrCl and $CHCl_2$,[15] CH_2Br and CH_2I,[16] CF_2Cl and $CFCl_2$,[33] C_2H_5 and *n*-C_3H_7,[34] *s*-C_4H_9,[35,36] and *i*-C_3H_7 and *t*-C_4H_9.[37] The line in the picture is an unweighted, linear least-squares fit to the data. The current results are indicated by star symbols.

The rates increase with the electron density in the radical site, but not with the looseness of the weakest bound electron (i.e., lower IE(R)).

The room temperature rate coefficients of the R + Cl_2 reactions also correlate fairly well with the electron affinity of the radical (R) (Figure 3b). The increasing electron affinity reduces the radical reactivity toward Cl_2. This may be understood in the following way. The higher the electron affinity of the radical, the more the radical holds the electron and does not share it with Cl_2, which also has high EA. Consequently the formation of the bond between the radical center and Cl_2 in the reaction can be hindered by the higher the electron affinity of the radical.

By inspection of the results presented in parts a and b of Figure 3, some general conclusions can be drawn. (i) Replacing hydrogen atoms with halogen atoms in an alkyl radical decreases the R + Cl_2 reaction rate coefficients. (ii) Lengthening the carbon chain at α-position to the radical center increases the R + Cl_2 rate coefficients. (iii) Branching at the α-position seems to have a stronger rate enhancing influence than just the carbon chain length but more studies with the isomeric radicals are needed to further clarify this issue.

As has been discussed above, Seetula et al.[15] studied the CH_2Cl + Cl_2 and CH_3CCl_2 + Cl_2 reaction transition states by ab initio calculations, together with other alkyl and halogenated alkyl radical reactions with Cl_2 and found that as the electron density of the radical center decreases, the transition state of the R + Cl_2 reaction becomes tighter. Compared to the other radicals in this study, the CH_3CHCl radical has higher electron density in the radical center due to the methyl group substitution and it would be interesting to have an ab initio calculation of the potential energy surface for the reaction path with the transition state.

Conclusion

Three chlorinated alkyl radical reactions with Cl_2 have been studied in direct time-resolved measurements. The measured rate coefficients for two of the reactions studied (CH_2Cl + Cl_2 and CH_3CCl_2 + Cl_2) show an interesting behavior as temperature is varied: a negative temperature dependence below a specific limiting temperature and a positive dependence on temperature above it. The CH_3CHCl + Cl_2 reaction behaves differently at these temperatures and has steep negative temperature dependence over the whole experimental range covered. Linear correlations of the determined rate coefficients against radical properties have been sought in order to gain understanding about the factors affecting radical reactivity in R + Cl_2 reactions. CH_2Cl_2, from the CH_2Cl + Cl_2 reaction, was the only observed product in the studied reactions.

Acknowledgment. R.S.T. and M.P.R. acknowledge the support from the CoE of the Academy of Finland.

References and Notes

(1) Tsang, W. *Combust. Sci. Technol.* **1990**, *74*, 99.

(2) Sander, S. P.; Friedl, R. R.; Ravishankara, A. R.; Golden, D. M.; Kolb, C. E.; Kurylo, M. J.; Molina, M. J.; Moortgat, G. K.; Keller-Rudek, H.; Finlayson-Pitts, B. J.; Wine, P. H.; Huie, R. E.; Orkin, V. L. Chemical Kinetics and Photochemical Data for Use in Stratospheric Modelling: Evaluation Number 15; Publication 06-2; National Aeronautics and Space Administration, Jet Propulsion Laboratory, California Institute of Technology: Pasadena, CA, 2006.

(3) Chiltz, G.; Goldfinger, P.; Huybrechts, G.; Martens, G.; Verbeke, G. *Chem. Rev.* **1963**, *63* (4), 355.

(4) Poutsma, M. In *Methods in Free-Radical Chemistry*; Huyser, E. S., Ed.; Marcel Dekker: New York, 1969; Vol. 1, pp 79−193.

(5) Benson, S. W. U.S. Patent No. 4,199,533, 1980.

(6) Senkan, M. S. *Chem. Eng. Prog.* **1987**, *83* (12), 58.

(7) Cormier, S. A.; Lomnicki, S.; Backes, W.; Dellinger, B. *Environ. Health Perspect.* **2006**, *114* (6), 810.

(8) Violi, A.; D'Anna, A.; D'Alessio, A. *Chemosphere* **2001**, *42*, 463.

(9) *Scientific Assessment of Ozone Depletion: 2006*, Global Ozone Research and Monitoring Project−Report No. 50; WMO (World Meteorological Organization): Geneva, Switzerland, 2007; 572 pp.

(10) (a) http://periodic.lanl.gov/elements/17.html, 28. 09. 2009. (b) http://en.wikipedia.org/wiki/Chlorine, 28. 09. 2009.

(11) http://www.health.state.ny.us/environmental/emergency/chemical_terrorism/chlorine_tech.htm; 30.09.2009.

(12) Wayne, R. P. *Chemistry of atmospheres*, 3rd ed.; Oxford University Press, Inc.: New York, 2000.

(13) Johnston, H. S.; Goldfinger, P. *J. Chem. Phys.* **1962**, *37*, 700.

(14) Bell, T. N.; Perkins, K. A.; Perkins, P. G. *J. Phys. Chem.* **1977**, *81*, 2610.

(15) Seetula, J. A. *J. Chem. Soc., Faraday Trans.* **1998**, *94*, 3561.

(16) Seetula, J. A.; Gutman, D.; Lightfoot, P. D.; Rayes, M. T.; Senkan, S. M. *J. Phys. Chem.* **1991**, *95*, 10688.

(17) Knyazev, V. D.; Bencsura, A.; Dubinsky, I. A.; Gutman, D.; Melius, C. F.; Senkan, S. M. *J. Phys. Chem.* **1995**, *99*, 230.

(18) Kaiser, E. W.; Rimai, L.; Schwab, E.; Lim, E. C. *J. Phys. Chem.* **1992**, *96*, 303.

(19) Kaiser, E. W.; Wallington, T. J. *J. Phys. Chem.* **1995**, *99*, 8669.

(20) Dobis, O.; Benson, S. W. *J. Phys. Chem. A* **2000**, *104*, 5503.

(21) Eskola, A. J.; Timonen, R. S. *Phys. Chem. Chem. Phys.* **2003**, *5*, 2557.

(22) Marston, G.; Monks, P. S.; Wayne, R. P. In *General Aspects of the Chemistry of Radicals*; Alfassi, Z. B.; Ed.; John Wiley & Sons Ltd.: New York, 1999; pp 429−471.

(23) Paltenghi, R.; Ogryzlo, E. A.; Bayes, K. D. *J. Phys. Chem.* **1984**, *88*, 2595.

(24) Pauling, L. *Nature of the Chemical Bond*, 3rd ed,; Cornell University Press: Ithaca, NY, 1960; pp 88−95.

(25) Allred, A. L. *J. Inorg. Nucl. Chem.* **1961**, *17*, 215.

(26) Thomas, T. D. *J. Am. Chem. Soc.* **1970**, *92*, 4184.

(27) Seetula, J. A.; Gutman, D. *J. Phys. Chem.* **1991**, *95*, 3626.

(28) Timonen, R. S.; Seetula, J. A.; Niiranen, J.; Gutman, D. *J. Phys. Chem.* **1991**, *95*, 4009.

(29) Linstrom, P. J.; Mallard, W. G. *NIST Chemistry Webbook, NIST Standard Reference Database Number 69, June 2005*,; National Institute of Standards and Technology: Gaithersburg, MD (http://webbook.nist.gov).

(30) Eskola, A. J.; Timonen, R. S.; Marshall, P.; Chesnokov, E. N.; Krasnoperov, L. N. *J. Phys. Chem. A* **2008**, *112*, 7391.

(31) Kaiser, E. W.; Wallington, T. J.; Hurley, M. D. *Int. J. Chem. Kinet.* **1995**, *27*, 205.

(32) DeMare, G. R.; Huybrechts, G. *Trans. Faraday Soc.* **1968**, *64*, 1311.

(33) Timonen, R. S.; Russell, J. J.; Gutman, D. *Int. J. Chem. Kinet.* **1986**, *18*, 1193.

(34) Eskola, A. J.; Lozovsky, V. A.; Timonen, R. S. *Int. J. Chem. Kin.* **2007**, *39*, 614.

(35) Tyndall, G. S.; Orlando, J. J.; Wallington, T. J.; Dill, M.; Kaiser, E. W. *Int. J. Chem. Kinet.* **1997**, *29*, 43.

(36) Lenhardt, T. M.; McDade, C. E.; Bayes, K. D. *J. Chem. Phys.* **1980**, *72*, 304.

(37) Timonen, R. S.; Gutman, D. *J. Phys. Chem.* **1986**, *90*, 2987.

(38) Born, M.; Ingemann, S.; Nibbering, N. M. M. *J. Am. Chem. Soc.* **1994**, *116*, 7210.

(39) Born, M.; Ingemann, S.; Nibbering, N. M. M. *Int. J. Mass Spectrom. Ion Processes* **2000**, *194*, 103.

(40) Eskola, A. J. PhD Thesis, University of Helsinki, Helsinki, 2007 (http://urn.fi/URN:ISBN:978-952-10-3786-3).

JP909419V